

Voltammetry of $[\text{Ru}_4\text{N}]_4[\text{M}_{18}\text{O}_{54}(\text{SO}_3)_2]$ and $[\text{Ru}(\text{bpy})_3]_2[\text{M}_{18}\text{O}_{54}(\text{SO}_3)_2]$ ($\text{M} = \text{Mo}, \text{W}$) as microcrystals adhered to a glassy carbon electrode surface in contact with ionic liquid media†

Monika Góral,^a Timothy McCormac,^{*b} Eithne Dempsey,^a De-Liang Long,^c Leroy Cronin^{*c} and Alan M. Bond^{*d}

Received 16th December 2008, Accepted 17th April 2009

First published as an Advance Article on the web 10th July 2009

DOI: 10.1039/b822167g

Based on studies with microcrystals of $[\text{Ru}(\text{bpy})_3]_2[\alpha\text{-W}_{18}\text{O}_{54}(\text{SO}_3)_2]$ adhered to an electrode surface in contact with the ionic liquids $[\text{BMIM}][\text{PF}_6]$ and $[\text{BMIM}][\text{BF}_4]$, it has been found that a series of well defined mono-electronic reduction processes associated with the tungsten-oxo cage of the $[\alpha\text{-W}_{18}\text{O}_{54}(\text{SO}_3)_2]^{4-}$ species are observed at much less negative potentials than found in conventional organic solvents. Furthermore, since the potentials of the $[\text{Ru}(\text{bpy})_3]^{2+}$ 2,2'-bipyridyl ligand based reduction processes are not strongly medium dependent, ionic liquid investigations allowed the characterisation of the $[\text{Ru}(\text{bpy})_3]_2[\alpha\text{-W}_{18}\text{O}_{54}(\text{SO}_3)_2]$ complex without extensive overlap of the ligand based reductions from the $[\text{Ru}(\text{bpy})_3]^{2+}$ cation and the $[\text{W}_{18}\text{O}_{54}(\text{SO}_3)_2]^{4-}$ anions. In the case of the Mo analogues, $[\alpha$ and $\beta\text{-Mo}_{18}\text{O}_{54}(\text{SO}_3)_2]^{4-}$, the much higher reactivity of the reduced forms precluded access to well defined mono-electronic reversible steps at negative potentials in all media examined, even though reduction is far easier and hence availability of extensively reduced species should be simpler, in a thermodynamic sense.

1.0 Introduction

Recently, a new class of sulfite polyoxometalate materials have been characterised.¹⁻⁴ These have novel structures,² and when dissolved in acetonitrile, exhibit an extensive series (at least five steps) of electron transfer reactions $[\alpha\text{-M}_{18}\text{O}_{54}(\text{SO}_3)_2]^{4-/-5/-6/-7/-8-}$ ($\text{M} = \text{W}, \text{Mo}$)^{1,3} when reduced electrochemically at glassy carbon electrodes. Studies with the two electron reduced sulfite based polyoxometalate in aqueous electrolyte, where proton coupling shifts the potential to less negative potentials, imply that an even more extensive series of one electron reduction processes should be available in aprotic media, if more negative potential ranges are accessible.⁴ The tungsten polyoxometalate also is reduced in the presence of light and a photo-sensitiser.³

Based on the above discussion and analogy with the sulfate Dawson $[\alpha\text{-M}_{18}\text{O}_{54}(\text{SO}_4)_2]^{4-}$ polyoxometallates,⁵ it may also be predicted that six or more electrons could be added to the sulfite polyoxometalates, provided a suitable electrochemical environment could be identified. Furthermore, alteration of the cation to the redox active and photoactive $[\text{Ru}(\text{bpy})_3]^{2+}$ species ($\text{bpy} = 2,2'\text{-bipyridyl}, \text{C}_{10}\text{H}_8\text{N}_2$) also might induce new elec-

trochemical and photochemical properties, as found in studies on $[\text{Ru}(\text{bpy})_3]_2[\alpha\text{-M}_{18}\text{O}_{54}(\text{SO}_4)_2]^{6-}$ and $[\text{Ru}(\text{bpy})_3]_3[\text{W}_{18}\text{O}_{54}(\text{PO}_4)_2]^{7-}$. Consequently, in this paper we report the synthesis of $[\text{Ru}(\text{bpy})_3]_2[\text{M}_{18}\text{O}_{54}(\text{SO}_3)_2]$ complexes and their electrochemistry as well as that of the parent $[\text{M}_{18}\text{O}_{54}(\text{SO}_3)_2]^{4-}$ compounds under a wide range of conditions to assess the full extent of electron transfer available in aprotic organic and ionic liquid solvent media.⁶

2.0 Experimental

2.1. Materials

$[\text{Bu}_4\text{N}]_4[\alpha\text{-W}_{18}\text{O}_{54}(\text{SO}_3)_2]$, $[\text{Pn}_4\text{N}]_4[\alpha\text{-Mo}_{18}\text{O}_{54}(\text{SO}_3)_2]$, $[\text{Bu}_4\text{N}]_4[\beta\text{-Mo}_{18}\text{O}_{54}(\text{SO}_3)_2]$, $[\text{Ru}(\text{bpy})_3][\text{BF}_4]$ and $[\text{Ru}(\text{bpy})_3][\text{PF}_6]$ were synthesised by literature methods.^{1,2,8,9} $[\text{Ru}(\text{bpy})_3]_2[\alpha\text{-W}_{18}\text{O}_{54}(\text{SO}_3)_2]$, $[\text{Ru}(\text{bpy})_3]_2[\alpha\text{-Mo}_{18}\text{O}_{54}(\text{SO}_3)_2]$ and $[\text{Ru}(\text{bpy})_3]_2[\beta\text{-Mo}_{18}\text{O}_{54}(\text{SO}_3)_2]$ were prepared according to procedures in Section 2.2. Biotech grade *N,N*-dimethylformamide, DMF (99.9+%, Aldrich) was used as supplied by the manufacturer. Voltammetric data obtained from this DMF source, were the same as obtained using purified, distilled DMF. Tetrabutylammonium hexafluorophosphate, Bu_4NPF_6 (GFS Chemicals) was recrystallized twice from ethanol before use and employed as the supporting electrolyte for electrochemical studies in DMF. Ferrocene (BDH Chemicals), cobaltocenium hexafluorophosphate (98%, Strem Chemicals), acetonitrile (Aldrich) and the ionic liquids 1-*n*-butyl-3-methylimidazolium tetrafluoroborate, $[\text{BMIM}][\text{BF}_4]$ (Merck, high purity) and hexafluorophosphate, $[\text{BMIM}][\text{PF}_6]$ (Merck, high purity) were used as received.

^aCentre for Research in Electroanalytical Technology "CREATE", Institute of Technology, Tallaght, Dublin, Department of Science, Dublin 24, Ireland

^bElectrochemistry Research Group, Dundalk Institute of Technology, Dublin Road, County Louth, Ireland. E-mail: tim.mccormac@dkit.ie

^cWestCHEM, Department of Chemistry, The University of Glasgow, Glasgow, UK G12 8QQ. E-mail: L.Cronin@chem.gla.ac.uk

^dSchool of Chemistry, Monash University, Clayton, Victoria 3800, Australia. E-mail: alan.bond@sci.monash.edu.au

† Electronic supplementary information (ESI) available: Fig. S1. See DOI: 10.1039/b822167g

2.2. Syntheses

Preparation of $[\text{Ru}(\text{bpy})_3]_2[\alpha\text{-W}_{18}\text{O}_{54}(\text{SO}_3)_2]$. $[\text{Pn}_4\text{N}]_4[\alpha\text{-W}_{18}\text{O}_{54}(\text{SO}_3)_2]$ (200 mg) was dissolved in CH_3CN (30 mL) and added to a solution of $[\text{Ru}(\text{bpy})_3][\text{BF}_4]_2$ (80 mg in 20 mL CH_3CN) under stirring. The mixture was stirred for further 5 min. The brown precipitate was filtered and washed with CH_3CN and dried in vacuum. Yield 120 mg. IR (KBr disk): ν/cm^{-1} : 3444, 1625, 1445, 969, 904, 785, 760, 729; elemental analysis (%) calcd. for $\text{C}_{60}\text{H}_{48}\text{Mo}_{18}\text{N}_{12}\text{O}_{60}\text{Ru}_2\text{S}_2$: C 18.52, H 1.24, N 4.32; found: C 18.62, H 1.30, N 4.39.

Preparation of $[\text{Ru}(\text{bpy})_3]_2[\beta\text{-Mo}_{18}\text{O}_{54}(\text{SO}_3)_2]$. $[\text{Ru}(\text{bpy})_3]_2[\beta\text{-Mo}_{18}\text{O}_{54}(\text{SO}_3)_2]$ was prepared using $[\text{Pn}_4\text{N}]_4[\beta\text{-Mo}_{18}\text{O}_{54}(\text{SO}_3)_2]$ in the same procedure as for $[\text{Ru}(\text{bpy})_3]_2[\alpha\text{-Mo}_{18}\text{O}_{54}(\text{SO}_3)_2]$. IR (KBr disk): ν/cm^{-1} : 3446, 1630, 1445, 970, 905, 787, 759, 728; elemental analysis (%) calcd. for $\text{C}_{60}\text{H}_{48}\text{Mo}_{18}\text{N}_{12}\text{O}_{60}\text{Ru}_2\text{S}_2$: C 18.52, H 1.24, N 4.32; found: C 18.59, H 1.28, N 4.35.

Preparation of $[\text{Ru}(\text{C}_{10}\text{H}_8\text{N}_2)_3]_2[\alpha\text{-W}_{18}\text{O}_{54}(\text{SO}_3)_2]$. $(\text{C}_{16}\text{H}_{36}\text{N})_4[\alpha\text{-W}_{18}\text{O}_{54}(\text{SO}_3)_2]$ (750 mg) was dissolved in CH_3CN (60 mL) and added to a solution of $[\text{Ru}(\text{bpy})_3][\text{BF}_4]_2$ (240 mg in 60 mL CH_3CN) under stirring. The mixture was stirred for further 5 min. The brown precipitate was filtered and washed with CH_3CN and dried in vacuum. Yield 600 mg. IR (KBr disk): ν/cm^{-1} : 3435, 1627, 1445, 992, 916, 876, 783, 755, 728; elemental analysis calcd. for $\text{C}_{60}\text{H}_{48}\text{W}_{18}\text{N}_{12}\text{O}_{60}\text{Ru}_2\text{S}_2$: C 13.17, H 0.88, N 3.07; found: C 13.11, H 0.93, N 3.11%.

2.3. Apparatus and procedures

Either BAS (Bioanalytical Systems) 100B or Epsilon Electrochemical Workstations were employed for cyclic voltammetric experiments. A three-electrode system was employed with a 1.0 mm diameter glassy carbon disk as the working electrode (GCE) and platinum wire for both the counter and quasi-reference electrodes. The reversible potential, for the Cc^+/Cc process, calculated from the average of the reduction and oxidation peak potentials, $((E_p^{\text{red}} + E_p^{\text{ox}})/2)$, obtained under conditions of cyclic voltammetry for the reduction of the cobaltocenium cation (Cc^+), was used as an internal potential reference scale. Potentials were corrected and quoted relative to the ferrocenium–ferrocene redox couple (Fc^+/Fc). Prior to each experiment, the working electrode was polished with alumina powder (0.3 μm), cleaned by sonication in distilled water and then dried. In the case of rotating disk electrode (RDE) voltammetry, experiments were carried out with a BAS RDE-2 assembly using a 3 mm diameter GCE and the same reference and auxiliary electrode as used in the cyclic voltammetric studies. To attach microcrystalline forms of the solids onto the electrode surface, the following procedure was employed. A drop of distilled water was added to the microcrystals which were then transferred onto the GCE surface as a paste. Prior to electrochemical studies, the coating was allowed to dry under a nitrogen atmosphere. All voltammetric experiments were undertaken at 20 (± 2) $^\circ\text{C}$. Each solution was degassed with nitrogen for at least 10 minutes to remove oxygen. Photochemical reduction of $[\text{Ru}(\text{bpy})_3]_2[\alpha\text{-W}_{18}\text{O}_{54}(\text{SO}_3)_2]$ was achieved under white light (312–700 nm) irradiation, which was introduced using a Polilight PL6 source (Rofin).

3.0 Results and discussion

3.1. Solution phase cyclic voltammetry of $[\text{Bu}_4\text{N}]_4[\alpha\text{-W}_{18}\text{O}_{54}(\text{SO}_3)_2]$ in DMF

In order to establish the solution phase redox chemistry of the $[\text{Ru}(\text{bpy})_3]_2[\alpha\text{-W}_{18}\text{O}_{54}(\text{SO}_3)_2]$ salt, it is important to define the processes associated with $[\text{Ru}(\text{bpy})_3]^{2+}$, added as the PF_6^- salt, and $[\alpha\text{-W}_{18}\text{O}_{54}(\text{SO}_3)_2]^{4-}$, added as the $[\text{Bu}_4\text{N}]^+$ salt, in the same solvent. Since $[\text{Ru}(\text{bpy})_3]_2[\alpha\text{-W}_{18}\text{O}_{54}(\text{SO}_3)_2]$ was found to be soluble in DMF, but only has very limited solubility in other commonly used electrochemical solvents such as acetonitrile, DMF was chosen for these initial comparative studies.

The solution phase voltammetry of $[\text{Bu}_4\text{N}]_4[\alpha\text{-W}_{18}\text{O}_{54}(\text{SO}_3)_2]$ (0.2 mM) in DMF (0.1 M Bu_4NPF_6) revealed two ideal chemically reversible one electron reduction waves (Fig. 1a, processes 1 and 2), followed by a third reasonably well defined one electron process (Fig. 1b, processes 3). At even more negative potentials, a fourth more complex and less reproducible reduction process, not shown, was detected. The first three processes correspond to the reduction of the tungsten polyoxometallate species as summarised in eqn (1).

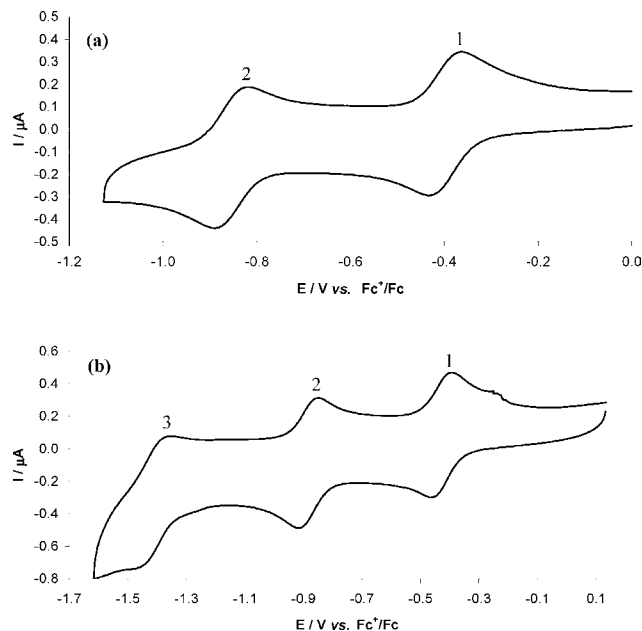
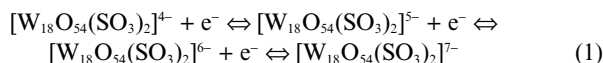


Fig. 1 Cyclic voltammetry (initial cycle of potential) obtained from 0.2 mM $[\text{Bu}_4\text{N}]_4[\alpha\text{-W}_{18}\text{O}_{54}(\text{SO}_3)_2]$ in DMF (0.1 M Bu_4NPF_6) at a GCE (diameter = 1 mm). Scan rate = 100 mV s^{-1} .

The high basicity of the very negatively charged species, $[\text{W}_{18}(\text{SO}_3)_2]^{7-}$, makes its electrochemistry very prone to the presence of adventitious water or other impurities that provide a source of protons which introduces complicated coupled electron and proton transfer. For this reason the fourth $[\alpha\text{-W}_{18}\text{O}_{54}(\text{SO}_3)_2]^{7-/8-}$ process is more complex and less reproducible in DMF. The reversible potential for this process given in Table 1 is therefore subject to considerably more uncertainty than for the initial three processes.

Table 1 Reversible potentials (E°) and peak to peak separations, ΔE_p , for $[\text{Bu}_4\text{N}]_4[\alpha\text{-W}_{18}\text{O}_{54}(\text{SO}_3)_2]$ (0.2 mM) in DMF (0.1 M Bu_4NPF_6) and $[\text{Pr}_4\text{N}]_4[\alpha\text{-W}_{18}\text{O}_{54}(\text{SO}_3)_2]$ (1 mM) in CH_3CN (0.1 M Hx_4NClO_4)^a obtained by cyclic voltammetry at a GCE using a scan rate of 100 mV s^{-1}

Redox process	E° /mV vs. Fc^+/Fc		ΔE_p /mV	
	DMF	CH_3CN^a	DMF	CH_3CN^a
$[\text{W}_{18}\text{O}_{54}(\text{SO}_3)_2]^{4-/-5-}$	-430	-357	60	60
$[\text{W}_{18}\text{O}_{54}(\text{SO}_3)_2]^{5-/-6-}$	-885	-760	65	65
$[\text{W}_{18}\text{O}_{54}(\text{SO}_3)_2]^{6-/-7-}$	-1415	-1295	80	80
$[\text{W}_{18}\text{O}_{54}(\text{SO}_3)_2]^{7-/-8-}$	-1890 ^b	-1693	^b	70
$[\text{W}_{18}\text{O}_{54}(\text{SO}_3)_2]^{8-/-9-}$	^c	-2131	^c	85

^a See ref. 3. ^b Subject to considerable uncertainty, see text for details. ^c Not detected in solvent window.

The E° (reversible potential) values, for the four redox couples detected in DMF, calculated from the average of the reduction and oxidation peak potentials, are listed in Table 1 and compared with the literature values³ derived from the $[\text{Pr}_4\text{N}]_4[\alpha\text{-W}_{18}\text{O}_{54}(\text{SO}_3)_2]$ salt dissolved in CH_3CN (0.1 M Hx_4NClO_4). Studies in CH_3CN displayed five one electron redox processes instead of four in the case of DMF (0.1 M Bu_4NPF_6). Furthermore E° values in DMF are considerably more negative than in acetonitrile. It is suggested that a fifth and perhaps an additional monoelectronic processes lie beyond the negative potential electrochemical window available in DMF (0.1 M Bu_4NPF_6). The values for peak to peak separation, ΔE_p , obtained for process 1, 2 and 3 (Table 1) are close to the theoretically expected value of 56 mV for an electrochemically reversible one electron charge transfer process at 20°C . Departure from the ideal value can be attributed predominantly to a small level of uncompensated resistance.

3.2 Cyclic voltammetry of adhered $[\text{Bu}_4\text{N}]_4[\alpha\text{-W}_{18}\text{O}_{54}(\text{SO}_3)_2]$ in contact with $[\text{BMIM}][\text{PF}_6]$ and $[\text{BMIM}][\text{BF}_4]$

Voltammograms obtained for the $[\text{Bu}_4\text{N}]_4[\alpha\text{-W}_{18}\text{O}_{54}(\text{SO}_3)_2]$ solid adhered to a GCE in contact with $[\text{BMIM}][\text{PF}_6]$ and $[\text{BMIM}][\text{BF}_4]$ are presented in Fig. 2a and 2b (second cycle shown), respectively. On the second and subsequent cycles of the potential, seven well defined, chemically reversible one-electron reduction processes (labelled 1–7) instead of four (only three well-defined) or five (only four well defined) processes detected with the salt dissolved in DMF (0.1 M Bu_4NPF_6) and CH_3CN (0.1 M Hx_4NClO_4), respectively, within the available potential window. It would appear that the one electron reduced $[\text{Bu}_4\text{N}]_4[\alpha\text{-W}_{18}\text{O}_{54}(\text{SO}_3)_2]$ solid rapidly dissolves in the ionic liquids in the first cycle of potential so that the second and subsequent cycles of potential represents solution phase rather than solid state voltammetry. Mechanistic details of this class of process have been described by Zhang *et al.*¹⁰ Consequently these seven solution phase redox processes may be summarised by the scheme below (eqn (2)). Peak to peak separations, ΔE_p , lie in the range of $120 (\pm 20)$ mV. These ΔE_p values are larger than theoretically expected for electrochemically reversible one electron charge transfer process. However, the ΔE_p values for the known reversible Cc^+/Cc process under the same conditions also are around 120 mV. Consequently, the broadening of the ΔE_p values is attributed to uncompensated resistance.¹¹ In the case of $[\text{BMIM}][\text{BF}_4]$, an additional process (labelled A) was also observed at about -1830 mV. However it was weak

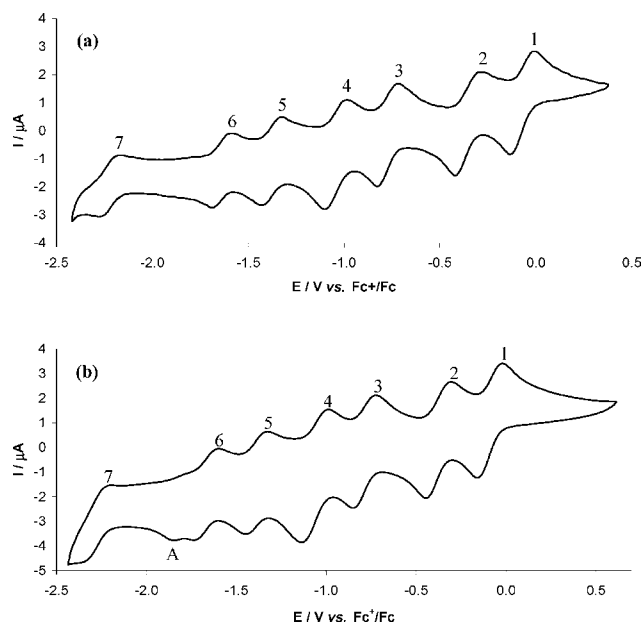
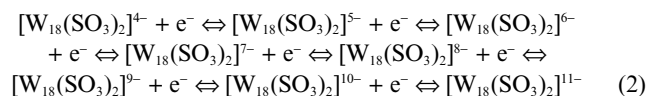


Fig. 2 Cyclic voltammograms (second cycle of potential) obtained for the reduction of $[\alpha\text{-W}_{18}\text{O}_{54}(\text{SO}_3)_2]^{4-}$ at a GCE (diameter = 1 mm) with a scan rate of 100 mV s^{-1} . Derived from adhered solid in contact with (a) $[\text{BMIM}][\text{PF}_6]$, (b) $[\text{BMIM}][\text{BF}_4]$.

and is attributed to the presence of protonated species derived from reaction of $[\text{W}_{18}\text{O}_{54}(\text{SO}_3)_2]^{10-}$, or other extensively reduced polyoxometallate, with water or other impurities.



The E° values for the seven reversible one electron processes are listed in Table 2. Values in $[\text{BMIM}][\text{BF}_4]$ are more positive than in DMF (by 330–820 mV) and CH_3CN (by 260–730 mV), Tables 1 and 2, with the differences becoming greater for the more negative processes. For $[\text{Bu}_4\text{N}]_4[\alpha\text{-W}_{18}\text{O}_{54}(\text{SO}_3)_2]$ in $[\text{BMIM}][\text{PF}_6]$, the E° values are slightly more negative than in $[\text{BMIM}][\text{BF}_4]$ by 20–60 mV. All seven processes in both ionic liquids were well-defined at scan rates in the range of $50\text{--}600 \text{ mV s}^{-1}$.

Two features stand out from examination of the reversible potentials in Table 2. Firstly, the potentials in the ionic liquids are hundreds of mV less negative than in organic solvents (Table 1). Several authors have commented^{12–22} on the dependence of polyoxometallate E° values upon the solvent and explained data in terms of permittivity, donor number and ion pairing. Such concepts are difficult to apply in the case of ionic liquid media but the large shift in E° values relative to organic solvents has been observed elsewhere.^{10,14} In our case we have been able to use adhered solids as a starting point to obtain solution phase reversible potentials and hence obtain new processes for the reduction of $[\alpha\text{-W}_{18}\text{O}_{54}(\text{SO}_3)_2]^{4-}$. Secondly it is noteworthy that a large gap exists between processes 6 and 7. For the first six processes a gap of about 300 mV occurs between processes 1 and 2, 3 and 4 and 5 and 6, with a larger gap of about 400 mV between processes 2 and 3 and 4 and 5. This pattern has been detected for the reduction of $[\alpha\text{-M}_{18}\text{O}_{54}(\text{SO}_4)_2]^{4-}$.¹⁰ In the present case, addition of the seventh electron appears to require a considerable amount of extra energy relative to the first to sixth electrons. This may arise

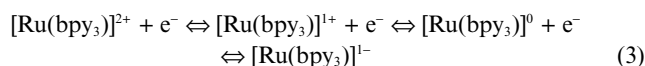
Table 2 Reversible potentials (E°) derived from voltammetry of $[\text{Bu}_4\text{N}]_4[\alpha\text{-W}_{18}\text{O}_{54}(\text{SO}_3)_2]$ and $[\text{Ru}(\text{bpy})_3]_2[\alpha\text{-W}_{18}\text{O}_{54}(\text{SO}_3)_2]$ adhered to the surface of GCE (diameter = 1 mm) in contact with $[\text{BMIM}][\text{BF}_4]$ and $[\text{BMIM}][\text{PF}_6]$. Scan rate = 100 mV s^{-1}

Redox process (labelled as)	E° [mV vs. Fc^+/Fc]			
	$[\text{Bu}_4\text{N}]_4[\alpha\text{-W}_{18}\text{O}_{54}(\text{SO}_3)_2]$		$[\text{Ru}(\text{bpy})_3]_2[\alpha\text{-W}_{18}\text{O}_{54}(\text{SO}_3)_2]$	
	$[\text{BMIM}][\text{BF}_4]$	$[\text{BMIM}][\text{PF}_6]$	$[\text{BMIM}][\text{BF}_4]$	$[\text{BMIM}][\text{PF}_6]$
$[\text{W}_{18}\text{O}_{54}(\text{SO}_3)_2]^{4-/5-}$ (1)	-95	-70	-80	-80
$[\text{W}_{18}\text{O}_{54}(\text{SO}_3)_2]^{5-/6-}$ (2)	-380	-350	-370	-375
$[\text{W}_{18}\text{O}_{54}(\text{SO}_3)_2]^{6-/7-}$ (3)	-790	-775	-780	-790
$[\text{W}_{18}\text{O}_{54}(\text{SO}_3)_2]^{7-/8-}$ (4)	-1070	-1045	-1040	-1050
$[\text{W}_{18}\text{O}_{54}(\text{SO}_3)_2]^{8-/9-}$ (5)	-1400	-1380	-1390	-1385
$[\text{W}_{18}\text{O}_{54}(\text{SO}_3)_2]^{9-/10-}$ (6)	-1670	-1640	—	—
$[\text{W}_{18}\text{O}_{54}(\text{SO}_3)_2]^{10-/11-}$ (7)	-2290	-2225	—	—
$[\text{Ru}(\text{bpy})_3]^{3+/2+}$ (I')	—	—	+900	+900
$[\text{Ru}(\text{bpy})_3]^{2+/1+}$ (I)	—	—	-1660	-1695
$[\text{Ru}(\text{bpy})_3]^{1+/0}$ (II)	—	—	-1825	-1845
$[\text{Ru}(\text{bpy})_3]^{0/1-}$ (III)	—	—	-2045	-2065

because the seventh electron is located on one of the 6 positions located in the cap regions (there are 12 positions in the belt regions which could easily accommodate 6 electrons such that no two electrons are located in adjacent sites).

3.3 Solution phase cyclic voltammetry of $[\text{Ru}(\text{bpy})_3][\text{PF}_6]_2$ in DMF

Fig. 3 illustrates a cyclic voltammogram recorded for 1 mM $[\text{Ru}(\text{bpy})_3][\text{PF}_6]_2$ in DMF (0.1 M Bu_4NPF_6). The expected $[\text{Ru}(\text{bpy})_3]^{2+/3+}$ metal-based oxidation process, labelled as I', and three bipyridyl ligand based reduction processes, labelled I, II and III, (eqn (3)) were observed. A further not fully reversible one electron reduction processes associated with the $[\text{Ru}(\text{bpy})_3]^{1-/2-}$ redox process was also present just prior to the solvent limit. The E° values for all processes are listed in Table 3 and agree with the literature.⁵ ΔE_p values obtained in this study are close to those theoretically expected for reversible one electron charge transfer processes.



Under very low temperature conditions of $-54 \text{ }^\circ\text{C}$ ²³ six reversible ligand based reduction processes have been reported when $[\text{Ru}(\text{bpy})_3]^{2+}$ is dissolved in DMF (0.1 M Et_4NPF_6). Data from this

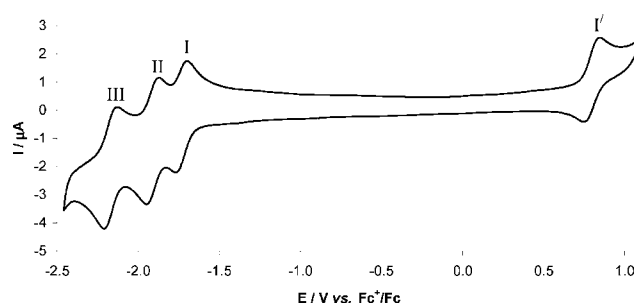


Fig. 3 Cyclic voltammetry (second cycle of potential) of 1 mM $[\text{Ru}(\text{bpy})_3][\text{PF}_6]_2$ in DMF (0.1 M Bu_4NPF_6) at GCE (diameter = 1 mm). Scan rate = 100 mV s^{-1} .

study are also included in Table 3 and agree well with the present data.

3.4 Cyclic voltammetry of adhered microcrystals of $[\text{Ru}(\text{bpy})_3][\text{PF}_6]_2$ in contact with $[\text{BMIM}][\text{PF}_6]$ and when dissolved in $[\text{BMIM}][\text{BF}_4]$

Fig. 4a, b and c depict cyclic voltammograms derived from the adhered $[\text{Ru}(\text{bpy})_3][\text{PF}_6]_2$ salt in contact with $[\text{BMIM}][\text{PF}_6]$. As in the case when the salt is dissolved in DMF (0.1 M Bu_4NPF_6), $\text{Ru}^{2+/3+}$ metal-based oxidation process, labelled as I', and a series of bipyridyl ligand based reduction processes, labelled as I, II, III,

Table 3 Reversible potentials (E°) for $[\text{Ru}(\text{bpy})_3][\text{PF}_6]_2$ obtained by cyclic voltammetry at a GCE (diameter = 1 mm) with a scan rate of 100 mV s^{-1} when the salt was dissolved in DMF/0.1 M Bu_4NPF_6 or in $[\text{BMIM}][\text{BF}_4]$ or adhered to the electrode surface in contact with $[\text{BMIM}][\text{PF}_6]$

Redox process (labelled as)	E° mV vs. Fc^+/Fc			
	Solution in DMF (0.1 M Et_4NPF_6) at $-54 \text{ }^\circ\text{C}$ ^a	1 mM soln. in DMF (0.1 M Bu_4NPF_6) at $20 \text{ }^\circ\text{C}$	1 mM soln. in $[\text{BMIM}][\text{BF}_4]$ at $20 \text{ }^\circ\text{C}$	Adhered solid in contact with $[\text{BMIM}][\text{PF}_6]$
$[\text{Ru}(\text{bpy})_3]^{3+/2+}$ (I')	—	+800	+900	+900
$[\text{Ru}(\text{bpy})_3]^{2+/1+}$ (I)	-1760	-1740	-1650	-1580
$[\text{Ru}(\text{bpy})_3]^{1+/0}$ (II)	-1920	-1910	-1830	-1750
$[\text{Ru}(\text{bpy})_3]^{0/1-}$ (III)	-2140	-2170	-2040	-1950
$[\text{Ru}(\text{bpy})_3]^{1-/2-}$ (IV)	-2780	-2570 ^b	-2332 ^c	-2310
$[\text{Ru}(\text{bpy})_3]^{2-/3-}$ (V)	-3000	—	—	-2560 ^d
$[\text{Ru}(\text{bpy})_3]^{3-/4-}$	-3300	—	—	—

^a See ref 23. ^b Close to solvent limit and not fully reversible. ^c Not reversible. ^d Peak potential for fully irreversible process.

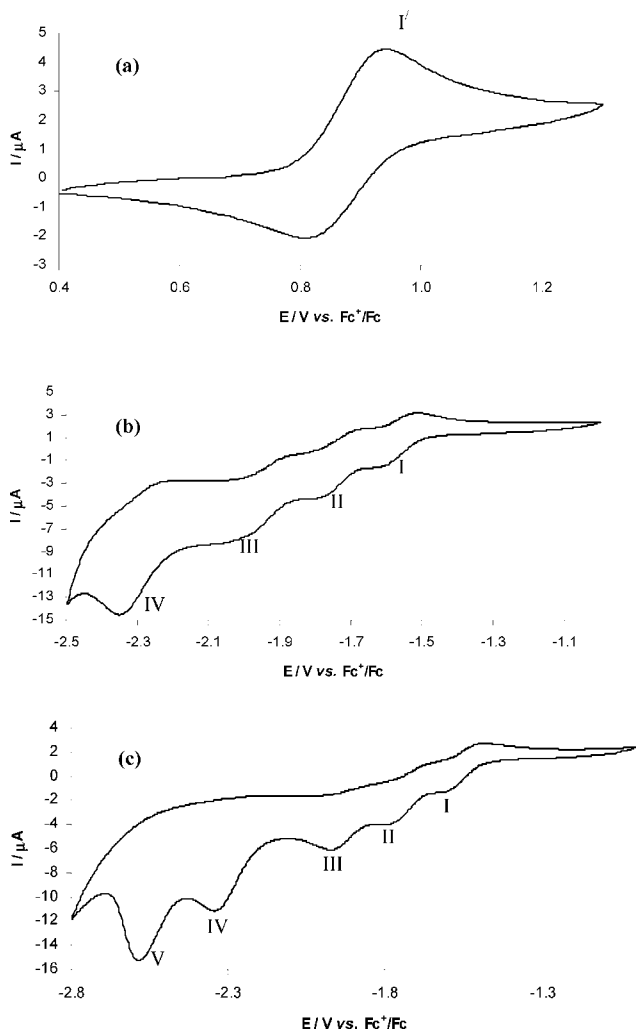


Fig. 4 Cyclic voltammograms (second cycle of potential) obtained at a scan rate of 100 mV s^{-1} for $[\text{Ru}(\text{bpy})_3][\text{PF}_6]_2$ adhered to a GCE (diameter = 1 mm) in contact with $[\text{BMIM}][\text{PF}_6]$. Curve (a) is for oxidation and (b) (c) for reduction with different switching potentials.

IV and V (Fig. 4c), were observed. Clearly, the voltammetry for this system based on adhered solid is not as well-defined as for the polyoxometallate systems. Zhang and Bond²⁴ have considered the theory for several different scenarios. Notably, the thickness of the layer, the kinetics of dissolution, and relative potentials of surface confined and solutions soluble processes and IR_u (ohmic) drop can all interplay in a complex manner. In this case the much larger currents give rise to increased IR_u drop, relative to that found with the polyoxometallate compounds. Nevertheless, since the first 4 reduction and the oxidation process have significant chemical reversibility, good estimates of reversible potentials for these processes can still be established. The fifth production process is chemically irreversible, so only a peak potential is available in this case. Reversible potentials are summarised in Table 3 and are more positive by about 100–260 mV (vs. Fc^+/Fc) in $[\text{BMIM}][\text{PF}_6]$ than found in DMF (0.1 M Bu_4NPF_6). As $[\text{Ru}(\text{bpy})_3][\text{PF}_6]_2$ was found to be soluble at the mM level in $[\text{BMIM}][\text{BF}_4]$, the solution phase voltammetry was investigated in this ionic liquid. Cyclic voltammograms recorded in a 1 mM solution of $[\text{Ru}(\text{bpy})_3][\text{PF}_6]_2$ in $[\text{BMIM}][\text{BF}_4]$ exhibited the expected $[\text{Ru}(\text{bpy})_3]^{2+/3+}$ metal-

based redox process and four bipyridyl ligand based reduction processes. Data are summarised in Table 3. The $E^{\circ'}$ values for the ligand based processes were less positive by about 100 mV than those obtained for the adhered salt in contact with $[\text{BMIM}][\text{PF}_6]$. The reversible potential for the metal based $[\text{Ru}(\text{bpy})_3]^{2+/3+}$ process, is similar in both ionic liquids.

3.5 Solution phase voltammetry of $[\text{Ru}(\text{bpy})_3]_2[\alpha\text{-W}_{18}\text{O}_{54}(\text{SO}_3)_2]$ in DMF

3.5.1. Cyclic voltammetry. Examination of cyclic voltammograms recorded for a 0.2 mM solution of $[\text{Ru}(\text{bpy})_3]_2[\alpha\text{-W}_{18}\text{O}_{54}(\text{SO}_3)_2]$ in DMF (0.1 M Bu_4NPF_6) established the presence of well-defined, reversible $[\text{Ru}(\text{bpy})_3]^{2+/3+}$, $[\alpha\text{-W}_{18}\text{O}_{54}(\text{SO}_3)_2]^{4-/5-}$ and $[\alpha\text{-W}_{18}\text{O}_{54}(\text{SO}_3)_2]^{5-/6-}$ redox processes (Fig. 5a and 5b respectively). The $[\alpha\text{-W}_{18}\text{O}_{54}(\text{SO}_3)_2]^{6-/7-}$ well defined process resembles that shown in Fig. 1b for the Bu_4N^+ salt of $[\alpha\text{-W}_{18}\text{O}_{54}(\text{SO}_3)_2]^{4-}$. The fourth process remains ill defined as was the case with the Bu_4N^+ salt. The ligand $[\text{Ru}(\text{bpy})_3]^{2+}$ based processes are seen at very negative potentials but are not as well defined as is the case with the $[\text{Ru}(\text{bpy})_3]\text{PF}_6$ salt (Fig. 3). The $E^{\circ'}$ value for the oxidation process was close to that obtained with $[\text{Ru}(\text{bpy})_3](\text{PF}_6)_2$ (Tables 3 and 4). The $[\alpha\text{-W}_{18}\text{O}_{54}(\text{SO}_3)_2]^{4-/5-/6-/7-}$ processes occur at slightly more negative potentials than when derived from the Bu_4N^+ salt (Tables 1 and 4). Finally it can be noted that bipyridyl ligand reduction processes are about 100 mV more negative than the data derived from the $[\text{Ru}(\text{bpy})_3](\text{PF}_6)_2$ salt (Tables 3 and 4). The $[\alpha\text{-W}_{18}\text{O}_{54}(\text{SO}_3)_2]^{7-/8-}$ process is difficult to detect even when obtained from the Bu_4N^+ salt and is also close to the bipyridyl ligand based reduction waves. Overlap of the polyoxometallate and bipyridyl ligand processes is less pronounced than in the case of $[\text{Ru}(\text{bpy})_3]_2[\text{Mo}_{18}\text{O}_{54}(\text{SO}_4)_2]$.⁵ The ΔE_p values (Table 4) are larger than theoretically expected for electrochemically reversible

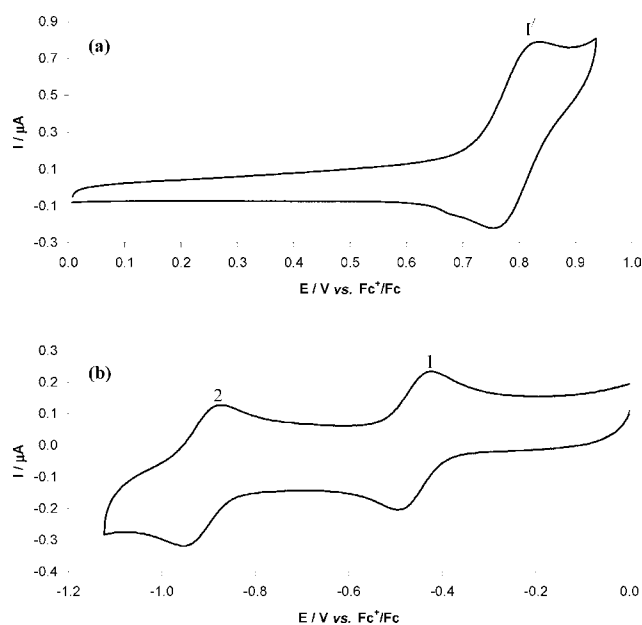


Fig. 5 Cyclic voltammetry (second cycle of potential) of 0.2 mM $[\text{Ru}(\text{bpy})_3]_2[\alpha\text{-W}_{18}\text{O}_{54}(\text{SO}_3)_2]$ in DMF (0.1 M Bu_4NPF_6) at a GCE (diameter = 1 mm). Scan rate = 100 mV s^{-1} , (a) the initial scan in the positive potential direction, (b) initial scan in the negative potential direction.

Table 4 Reversible potentials ($E^{o'}$) and peak to peak separation, ΔE_p , for $[\text{Ru}(\text{bpy})_3]_2[\alpha\text{-W}_{18}\text{O}_{54}(\text{SO}_3)_2]$ (0.2 mM) in DMF (0.1 M Bu_4NPF_6) obtained by cyclic voltammetry at a GCE (diameter = 1 mm). Scan rate = 100 mV s^{-1}

Redox process (labelled as)	$E^{o'}/\text{mV vs. Fc}^+/ \text{Fc}$	$\Delta E_p/\text{mV}$
$[\text{W}_{18}\text{O}_{54}(\text{SO}_3)_2]^{4-/-5-}$ (1)	-455	65
$[\text{W}_{18}\text{O}_{54}(\text{SO}_3)_2]^{5-/-6-}$ (2)	-910	80
$[\text{W}_{18}\text{O}_{54}(\text{SO}_3)_2]^{6-/-7-}$ (3)	-1340	170
$[\text{Ru}(\text{bpy})_3]^{3+/2+}$ (I')	+795	70
$[\text{Ru}(\text{bpy})_3]^{2+/1+}$ (I)	-1820	145
$[\text{Ru}(\text{bpy})_3]^{1+/0}$ (II)	-2175	80
$[\text{Ru}(\text{bpy})_3]^{0/1-}$ (III)	-2630 ^a	—

^a peak potential for irreversible process.

one electron charge transfer process. However, again this can be attributed predominantly to uncompensated resistance.¹¹

With respect to current magnitude, it can be noted from examination of Fig. 5 that the peak currents for the ruthenium processes are much larger than for the polyoxometalate ones. A fully dissociated 0.2 mM solution of $[\text{Ru}(\text{bpy})_3]_2[\alpha\text{-W}_{18}\text{O}_{54}(\text{SO}_3)_2]$ contains 0.4 mM $[\text{Ru}(\text{bpy})_3]^{2+}$ and 0.2 mM $[\alpha\text{-W}_{18}\text{O}_{54}(\text{SO}_3)_2]^{4-}$. Thus, part of the reason for the larger ruthenium current is related to the higher concentration. However, the diffusion coefficient for the $[\text{Ru}(\text{bpy})_3]^{2+}$ cation is considerably larger than for the $[\alpha\text{-W}_{18}\text{O}_{54}(\text{SO}_3)_2]^{4-}$ anion. This leads to even further amplification of the ruthenium processes relative to the polyoxometalate ones.

3.5.2. Rotating disk voltammetry and photoelectrochemical properties of $[\text{Ru}(\text{bpy})_3]_2[\alpha\text{-W}_{18}\text{O}_{54}(\text{SO}_3)_2]$ in DMF (0.1 M Bu_4NPF_6). As the first two monoelectronic metal-oxygen reduction processes were well-defined for the $[\text{Ru}(\text{bpy})_3]_2[\alpha\text{-W}_{18}\text{O}_{54}(\text{SO}_3)_2]$ complex, the RDE technique was applied to these processes. Fig. 6 shows the RDE voltammogram for the $[\alpha\text{-W}_{18}\text{O}_{54}(\text{SO}_3)_2]^{4-/-5-}$ reduction processes. The half wave ($E_{1/2}$) potentials, that represent the potential where the current is half of the limiting value, are in good agreement with the $E^{o'}$ values calculated from cyclic voltammetry, as expected theoretically for a reversible process.

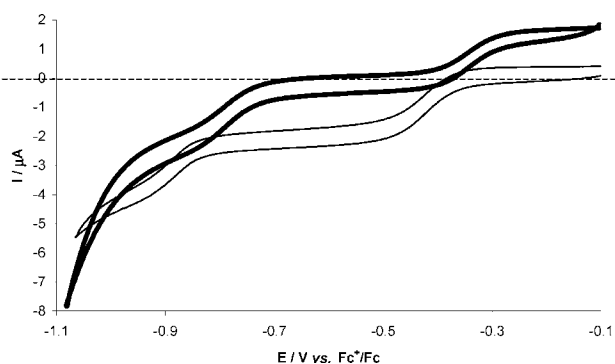


Fig. 6 GCE rotating disk (diameter = 3 mm) voltammograms recorded at a rotation rate of 500 rpm for the first two tungsten-oxo redox processes of $[\text{Ru}(\text{bpy})_3]_2[\alpha\text{-W}_{18}\text{O}_{54}(\text{SO}_3)_2]$ (0.2 mM) in DMF (0.1 M Bu_4NPF_6) before photoradiation (thin line) and after addition of 10% benzyl alcohol and irradiation with white light for 30 minutes (bold line).

It is known that photoexcited states of many polyoxometalate anions can be used to photooxidise organic compounds such as benzyl alcohol and generate reduced forms of the polyoxometalate anions.^{6,25-28} In an earlier study³ it was shown that the

$[\alpha\text{-W}_{18}\text{O}_{54}(\text{SO}_3)_2]^{4-}$ is photoactive. In this paper the photochemical properties of the $[\text{Ru}(\text{bpy})_3]_2[\alpha\text{-W}_{18}\text{O}_{54}(\text{SO}_3)_2]$ complex have been investigated. Photochemical reduction of this compound under white light irradiation in DMF (0.1 M Bu_4NPF_6) containing 10% benzyl alcohol was verified electrochemically by RDE voltammetry. Ruether *et al.*²⁵ demonstrated that benzyl alcohol was photooxidised to benzaldehyde in the presence of $[\text{Mo}_{18}\text{O}_{54}(\text{SO}_4)_2]^{4-}$ which was multiply reduced. In the case of $[\text{Ru}(\text{bpy})_3]_2[\alpha\text{-W}_{18}\text{O}_{54}(\text{SO}_3)_2]$ solution, in the presence of 10% benzyl alcohol and upon irradiation by white light for 30 minutes, the colour of the solution changed from red-orange to green-orange. The green colour suggests that the polyoxometalate anion has been reduced. Reduced polyoxometalates are blue. However in the presence of the orange colour from the ruthenium cation, the solution is expected to be green-orange. The photo-reduction reaction is confirmed by noting the change in the RDE voltammograms before and after irradiation with light (Fig. 6). The change in the position of zero current from negative, when $[\text{W}_{18}\text{O}_{54}(\text{SO}_4)_2]^{4-}$ is reduced, to positive, when $[\text{W}_{18}\text{O}_{54}(\text{SO}_4)_2]^{5-}$ is oxidised, confirmed that the one electron reduction of the $[\alpha\text{-W}_{18}\text{O}_{54}(\text{SO}_3)_2]^{4-}$ anion had occurred under these conditions. Additionally the $E_{1/2}$ values shifted to less negative potentials, because of the generation of protons.²⁵ These results show that $[\text{Ru}(\text{bpy})_3]_2[\alpha\text{-W}_{18}\text{O}_{54}(\text{SO}_3)_2]$ is an excellent photo-oxidant.

3.6 Cyclic voltammetry of adhered microcrystals of $[\text{Ru}(\text{bpy})_3]_2[\alpha\text{-W}_{18}\text{O}_{54}(\text{SO}_3)_2]$ in contact with $[\text{BMIM}][\text{PF}_6]$ and $[\text{BMIM}][\text{BF}_4]$

Fig. 7 illustrates cyclic voltammograms (second cycle of potential) recorded when $[\text{Ru}(\text{bpy})_3]_2[\alpha\text{-W}_{18}\text{O}_{54}(\text{SO}_3)_2]$ solid is adhered to the GCE surface in contact with $[\text{BMIM}][\text{PF}_6]$ and $[\text{BMIM}][\text{BF}_4]$. Analysis of these voltammograms established a well defined $[\text{Ru}(\text{bpy})_3]^{2+/3+}$ metal-based redox couple, again labelled as I', with an $E^{o'}$ value close to that obtained in the absence of

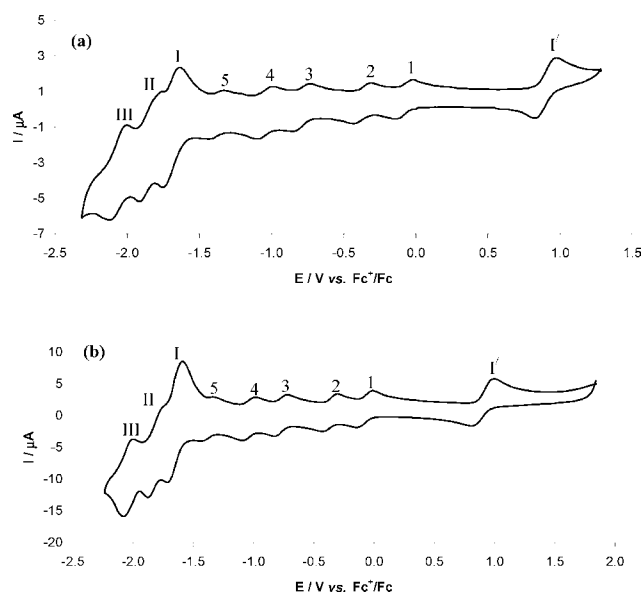


Fig. 7 Cyclic voltammograms (second cycle of potential) obtained for $[\text{Ru}(\text{bpy})_3]_2[\alpha\text{-W}_{18}\text{O}_{54}(\text{SO}_3)_2]$ at a GCE (diameter = 1 mm) with scan rate = 100 mV s^{-1} ; (a) adhered solid in contact with $[\text{BMIM}][\text{PF}_6]$, (b) adhered solid in contact with $[\text{BMIM}][\text{BF}_4]$.

$[\alpha\text{-W}_{18}\text{O}_{54}(\text{SO}_3)_2]^{4-}$ (Tables 2 and 3). Five well-defined, reversible reduction waves, corresponding to the tungsten-oxo redox processes (labelled 1 to 5) were also observed. Their E° values are similar to those obtained for $[\text{Bu}_4\text{N}]_4[\alpha\text{-W}_{18}\text{O}_{54}(\text{SO}_3)_2]$ under the same conditions (Table 2) and ΔE_p values again lie in the range of 120 (± 20) mV.

The detection of five tungsten-oxo redox processes represents a significant improvement in the voltammetry, compared to that found when $[\text{Ru}(\text{bpy})_3]_2[\alpha\text{-W}_{18}\text{O}_{54}(\text{SO}_3)_2]$ is dissolved in DMF (0.1 Bu_4NPF_6), where only the first three processes were well-defined. At the very negative region of potential, three other redox processes (labelled as I, II and III) are also present, which exhibit very similar potentials to those found for the bipyridyl ligand based reduction processes observed in the absence of $[\alpha\text{-W}_{18}\text{O}_{54}(\text{SO}_3)_2]^{4-}$ (Table 3). Consequently these three processes are defined as ligand based reductions of the $[\text{Ru}(\text{bpy})_3]^{2+}$ ion (Table 2). The current magnitudes for the ruthenium processes are again much larger than for the polyoxometalate reduction ones because of the higher concentration present after dissolution and also because of differences in diffusion coefficients. Examination of data in Tables 2 and 3 suggests that overlap of processes summarised in eqn (3) and those for the $[\alpha\text{-W}_{18}\text{O}_{54}(\text{SO}_3)_2]^{9-/10-}$ and $[\alpha\text{-W}_{18}\text{O}_{54}(\text{SO}_3)_2]^{10-/11-}$ processes occurs in this potential range, but the ruthenium processes dominate, because of the much larger diffusion coefficient and higher concentration.

Voltammograms derived from $[\text{Ru}(\text{bpy})_3]_2[\alpha\text{-W}_{18}\text{O}_{54}(\text{SO}_3)_2]$ in both $[\text{BMIM}][\text{PF}_6]$ and $[\text{BMIM}][\text{BF}_4]$ ionic liquids have similar characteristics, and are extremely well defined in the scan rate range of 50 to 600 mV s^{-1} . In the case of $[\text{BMIM}][\text{BF}_4]$ as the ionic liquid, processes are not as well resolved with slow scan rates of 10 or 20 mV s^{-1} as noted with the voltammetry of adhered $[\text{Bu}_4\text{N}]_4[\alpha\text{-W}_{18}\text{O}_{54}(\text{SO}_3)_2]$ solid.

3.7 Cyclic voltammetry of $[\text{Pn}_4\text{N}]_4[\alpha\text{-Mo}_{18}\text{O}_{54}(\text{SO}_3)_2]$ and $[\text{Bu}_4\text{N}]_4[\beta\text{-Mo}_{18}\text{O}_{54}(\text{SO}_3)_2]$

On the basis of the data obtained with microcrystals of the $[\text{Mo}_{18}\text{O}_{54}(\text{SO}_3)_2]^{4-}$ system, in ionic liquids, it could be anticipated that an extensive series of one electron processes could be found for the molybdenum analogue. To determine if this was the case, the two isomers, α and β , of $[\text{R}_4\text{N}]_4[\text{Mo}_{18}\text{O}_{54}(\text{SO}_3)_2]$ were investigated, namely in the form of $[\text{Pn}_4\text{N}]_4[\alpha\text{-Mo}_{18}\text{O}_{54}(\text{SO}_3)_2]$ and $[\text{Bu}_4\text{N}]_4[\beta\text{-Mo}_{18}\text{O}_{54}(\text{SO}_3)_2]$.

The solution phase voltammetry in DMF revealed two ideal chemically reversible one electron reduction waves for both isomers (eqn (4)). The ΔE_p values, for both isomers, obtained for process 1 and 2 lie in the range of 80 (± 20) mV which are close to the literature values.¹ This departure from the ideal value of 56 mV for electrochemically reversible one electron charge transfer process again is attributed to uncompensated resistance as the ΔE_p values for the known reversible Cc^+/Cc process under the same conditions is 70 mV. The third reduction step is consistent with $\beta \rightleftharpoons \alpha$ isomerisation associated with the $[\text{Mo}_{18}\text{O}_{54}(\text{SO}_3)_2]^{7-}$. At more negative potentials a series of complex and not highly reproducible processes are observed that imply $[\text{Mo}_{18}\text{O}_{54}(\text{SO}_3)_2]^{7-}$ is very sensitive to protonation arising from the presence of adventitious water and/or other impurities present in DMF.

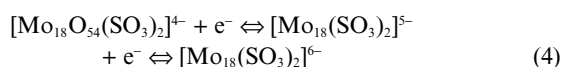


Table 5 Reversible potentials (E°) obtained for the α and β forms of $[\text{R}_4\text{N}]_4[\text{Mo}_{18}\text{O}_{54}(\text{SO}_3)_2]$ (R = Bu, Pn) (0.2 mM) in DMF (0.1 M Bu_4NPF_6) and in CH_3CN (0.1 M Hx_4NClO_4)^a by cyclic voltammetry at a GCE at a scan rate of 100 mV s^{-1}

Redox process (labelled as)	$E^{\circ}/\text{mV vs. Fc}^+/\text{Fc}$			
	$[\text{Pn}_4\text{N}]_4[\alpha\text{-Mo}_{18}\text{O}_{54}(\text{SO}_3)_2]$		$[\text{R}_4\text{N}]_4[\beta\text{-Mo}_{18}\text{O}_{54}(\text{SO}_3)_2]$ R = Bu or R = Pn ^a	
	DMF	CH_3CN^a	DMF	CH_3CN^a
$[\text{Mo}_{18}\text{O}_{54}(\text{SO}_3)_2]^{4-/5-}$ (1)	-70	-5	-105	-30
$[\text{Mo}_{18}\text{O}_{54}(\text{SO}_3)_2]^{5-/6-}$ (2)	-395	-265	-445	-310
$[\text{Mo}_{18}\text{O}_{54}(\text{SO}_3)_2]^{6-/7-}$ (3)	^b	-885	^b	-880
$[\text{Mo}_{18}\text{O}_{54}(\text{SO}_3)_2]^{7-/8-}$ (4)	—	-1195	—	-1180
$[\text{Mo}_{18}\text{O}_{54}(\text{SO}_3)_2]^{8-/9-}$ (5)	—	-1695	—	-1660
$[\text{Mo}_{18}\text{O}_{54}(\text{SO}_3)_2]^{9-/10-}$	—	-2075	—	-2030

^a See ref. 1. ^b Subject to considerable uncertainty, due to $\beta \rightleftharpoons \alpha$ isomerisation and reactions of $[\text{Mo}_{18}\text{O}_{54}(\text{SO}_3)_2]^{7-}$, see text for details.

The E° values for the two well defined reversible processes detected in DMF are listed in Table 5 and compared with the literature data¹ derived from the $[\text{Pn}_4\text{N}]_4[\alpha\text{-Mo}_{18}\text{O}_{54}(\text{SO}_3)_2]$ and $[\text{Pn}_4\text{N}]_4[\beta\text{-Mo}_{18}\text{O}_{54}(\text{SO}_3)_2]$ salts dissolved in CH_3CN (0.1 M Hx_4NClO_4). Studies in CH_3CN revealed the presence of an extensive series of six mono-electronic reduction processes (Table 5). The implications are that DMF provides a more reactive medium than acetonitrile and the reduced molybdenum polyoxometallates are much more reactive than the tungsten analogues.

Cyclic voltammograms for the α and β isomers of $[\text{Mo}_{18}\text{O}_{54}(\text{SO}_3)_2]^{4-}$, adhered to the electrode surface¹ have been shown to exhibit three well defined, mono-electronic, reversible molybdenum-oxo reduction waves, labelled 1–3, when in contact with $[\text{BMIM}][\text{PF}_6]$ instead of only two well-defined processes detected with dissolved salts in DMF (0.1 M Bu_4NPF_6).¹ There were a number of other molybdenum-oxo redox processes found at more negative potentials but these were of variable current magnitude and more complex. Furthermore, except for the initial process, the potentials were dependent on water and impurities present in the ionic liquid and potentials varied by up to 50 mV.

A slightly more extensive series of one electron reduction processes were obtained from $[\alpha\text{-Mo}_{18}\text{O}_{54}(\text{SO}_3)_2]^{4-}$ (Fig. 8) and $[\beta\text{-Mo}_{18}\text{O}_{54}(\text{SO}_3)_2]^{4-}$ microcrystals adhered to the GCE in contact with $[\text{BMIM}][\text{BF}_4]$ (Table 6). Voltammograms now exhibited four well defined reversible reduction waves. The data for both isomers are summarised in Table 6. Again additional processes were detected at more negative potentials in the $[\text{BMIM}][\text{BF}_4]$

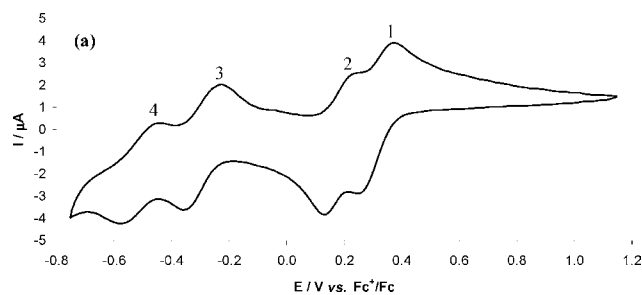


Fig. 8 Cyclic voltammograms (second cycle of potential) obtained for the reduction of $[\text{Pn}_4\text{N}]_4[\text{Mo}_{18}\text{O}_{54}(\text{SO}_3)_2]$ adhered to the surface of a GCE (diameter = 1 mm) in contact with $[\text{BMIM}][\text{BF}_4]$. Scan rate = 100 mV s^{-1} .

Table 6 Reversible potentials (E°) derived from voltammetry of α and β form of $[\text{RN}_4][\text{Mo}_{18}\text{O}_{54}(\text{SO}_3)_2]$ ($\text{R} = \text{Bu}, \text{Pn}$) adhered to the surface of a GCE (diameter = 1 mm) in contact with $[\text{BMIM}][\text{BF}_4]$ and $[\text{BMIM}][\text{PF}_6]$. Scan rate 100 mV s^{-1}

Redox process (labelled as)	$E^{\circ}/\text{mV vs. Fc}^+/\text{Fc}$ [BMIM][BF ₄]	
	[Pn ₄ N] ₄ [α - Mo ₁₈ O ₅₄ (SO ₃) ₂]	[Bu ₄ N] ₄ [β - Mo ₁₈ O ₅₄ (SO ₃) ₂]
$[\text{M}_{18}\text{O}_{54}(\text{SO}_3)_2]^{4+/-}$ (1)	+310 (+325) ^a	+255 (+310) ^a
$[\text{M}_{18}\text{O}_{54}(\text{SO}_3)_2]^{5-/-}$ (2)	+180 (+200) ^a	+105 (+175) ^a
$[\text{M}_{18}\text{O}_{54}(\text{SO}_3)_2]^{6-/-}$ (3)	-295 (-210) ^a	-330 (-260) ^a
$[\text{M}_{18}\text{O}_{54}(\text{SO}_3)_2]^{6-/-}$ (4)	-520	-530

^a see ref. 1

experiments, but they were of variable current magnitude and non reproducible. The E° values for the first three processes were similar to those obtained previously in $[\text{BMIM}][\text{PF}_6]$.

Several features emerge from examination of the voltammetric data. Thus, (a) the potentials in the two ionic liquids for both α and β - $[\text{Mo}_{18}\text{O}_{54}(\text{SO}_3)_2]^{4+}$ ion isomers, are hundreds of mV less negative than in DMF (Table 5), as was the case with α - $[\text{W}_{18}\text{O}_{54}(\text{SO}_3)_2]^{4+}$, (b) difference in E° values in DMF and CH_3CN organic solvents (0.1 M Bu_4NPF_6) are smaller and (c) potentials for reduction of the α isomer are less negative than for the β isomer in a wide range of media. However a major difference to the W analogue is the very high level of reactions of the reduced Mo polyoxometalates. Thus, even though the Mo salts are more easily reduced than the W one, as commonly reported in the polyoxometalate literature,¹⁰ more extensive reversible reduction is not easily achieved, even with use of ionic liquids.

Voltammograms recorded for 0.2 mM solutions of the α and β forms of $[\text{Ru}(\text{bpy})_3]_2[\text{Mo}_{18}\text{O}_{54}(\text{SO}_3)_2]$ in DMF (0.1 M Bu_4NPF_6) established the presence of well-defined, reversible $[\text{Ru}(\text{bpy})_3]^{2+/3+}$ and $[\text{Mo}_{18}\text{O}_{54}(\text{SO}_3)_2]^{4+/-}$ and $[\text{Mo}_{18}\text{O}_{54}(\text{SO}_3)_2]^{5-/-}$ processes (labelled I', 1 and 2, respectively in Fig. S1 in the Electronic Supplementary Information, ESI, for the β isomer).[†] The $[\text{Mo}_{18}\text{O}_{54}(\text{SO}_3)_2]^{6-/-}$ process for both isomers was also clearly seen but not the $[\text{Mo}_{18}\text{O}_{54}(\text{SO}_3)_2]^{7-/-}$ one. The bipyridyl ligand based processes were well defined. The E° value for the $[\text{Ru}(\text{bpy})_3]^{2+/3+}$ oxidation process, was close to that obtained from $[\text{Ru}(\text{bpy})_3][\text{PF}_6]_2$. Bipyridyl ligand based reduction processes were slightly more negative than when data were derived from the $[\text{Ru}(\text{bpy})_3][\text{PF}_6]_2$ salt (Tables 3 and 7). It can be also noted that the $[\text{Mo}_{18}\text{O}_{54}(\text{SO}_3)_2]^{4+/-}$ processes for both isomers were slightly more positive when derived from the R_4N^+ salts (Tables 5 and 6). Moreover, overlap of the polyoxometalate and bipyridyl ligand processes was much less pronounced than in the case of the $[\text{Ru}(\text{bpy})_3]_2[\alpha\text{-W}_{18}\text{O}_{54}(\text{SO}_3)_2]$ and $[\text{Ru}(\text{bpy})_3]_2[\text{Mo}_{18}\text{O}_{54}(\text{SO}_3)_2]$.⁵ In a similar manner to the $[\text{Ru}(\text{bpy})_3]_2[\alpha\text{-W}_{18}\text{O}_{54}(\text{SO}_3)_2]$ complex, it is evident from Fig. S1,[†] that the current magnitudes for the ruthenium process is much larger than for the polyoxometalate one.⁵ This can be ascribed again to the higher concentration present, after dissolution, and also because of differences in diffusion coefficients.

The voltammetry of the $[\text{Ru}(\text{bpy})_3]_2[\alpha\text{-Mo}_{18}\text{O}_{54}(\text{SO}_3)_2]$ (Fig. 9) and $[\text{Ru}(\text{bpy})_3]_2[\beta\text{-Mo}_{18}\text{O}_{54}(\text{SO}_3)_2]$ (Fig. 10) solids adhered to the GCE electrode surface in contact with $[\text{BMIM}][\text{PF}_6]$ established a well defined $[\text{Ru}(\text{bpy})_3]^{2+/3+}$ metal-based redox couple, again

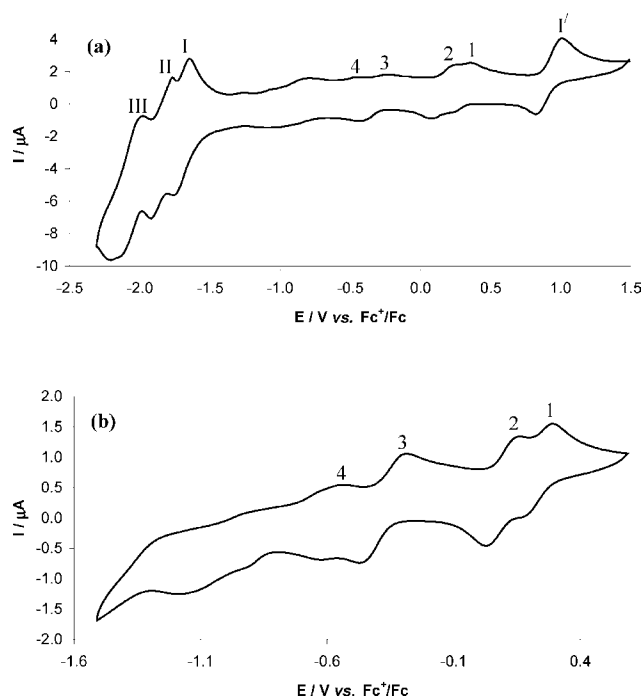


Fig. 9 Cyclic voltammograms (second cycle of potential) obtained for $[\text{Ru}(\text{bpy})_3]_2[\alpha\text{-Mo}_{18}\text{O}_{54}(\text{SO}_3)_2]$ adhered to the surface of a GCE (diameter = 1 mm) in contact with $[\text{BMIM}][\text{PF}_6]$. Scan rate = 100 mV s^{-1} .

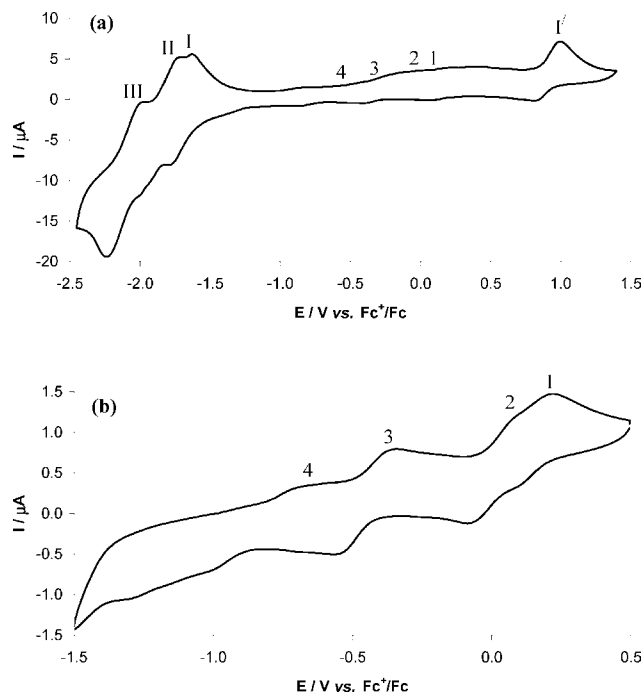


Fig. 10 Cyclic voltammograms (second cycle of potential) obtained for $[\text{Ru}(\text{bpy})_3]_2[\beta\text{-Mo}_{18}\text{O}_{54}(\text{SO}_3)_2]$ adhered to the surface of a GCE (diameter = 1 mm) in contact with $[\text{BMIM}][\text{PF}_6]$. Scan rate = 100 mV s^{-1} .

labelled as I', with E° values close to that obtained in the absence of $[(\alpha\text{- or } \beta\text{-})\text{Mo}_{18}\text{O}_{54}(\text{SO}_3)_2]^{4+}$ (Tables 7 and 3). These reversible reduction waves, corresponding to the molybdenum-oxo redox processes, labelled 1 to 3, were also observed. Their E° values were about 100 mV more negative than those obtained

Table 7 Reversible potentials (E°) for $[\text{Ru}(\text{bpy})_3]_2[\text{Mo}_{18}\text{O}_{54}(\text{SO}_3)_2]$ salts (α and β form) obtained by cyclic voltammetry at a GCE (diameter = 1 mm) with a scan rate of 100 mV s^{-1} when the salt was dissolved in DMF/0.1 M Bu_4NPF_6 or adhered to the electrode surface in contact with $[\text{BMIM}][\text{PF}_6]$

Redox process (labelled as)	$E^{\circ}/\text{mV vs. Fc}^+/\text{Fc}$			
	$[\text{Ru}(\text{bpy})_3]_2[\alpha\text{-Mo}_{18}\text{O}_{54}(\text{SO}_3)_2]$		$[\text{Ru}(\text{bpy})_3]_2[\beta\text{-Mo}_{18}\text{O}_{54}(\text{SO}_3)_2]$	
	0.2 mM solut. in DMF (0.1 M Bu_4NPF_6)	Adhered solid in contact with $[\text{BMIM}][\text{PF}_6]$	0.2 mM solut. in DMF (0.1 M Bu_4NPF_6)	Adhered solid in contact with $[\text{BMIM}][\text{PF}_6]$
$[\text{M}_{18}\text{O}_{54}(\text{SO}_3)_2]^{4-/-5-}$ (1)	-80	+235	-105	+160
$[\text{M}_{18}\text{O}_{54}(\text{SO}_3)_2]^{5-/-6-}$ (2)	-375	+90	-425	+100
$[\text{M}_{18}\text{O}_{54}(\text{SO}_3)_2]^{6-/-7-}$ (3)	-610	-380	-760	-455
$[\text{M}_{18}\text{O}_{54}(\text{SO}_3)_2]^{7-/-8-}$ (4)	—	-590	—	-845
$[\text{Ru}(\text{bpy})_3]^{3+/2+}$ (I')	+815	+915	+805	+910
$[\text{Ru}(\text{bpy})_3]^{2+/1+}$ (I)	-1790	-1705	-1730	-1710
$[\text{Ru}(\text{bpy})_3]^{1+/0}$ (II)	-1975	-1850	-1920	-1865
$[\text{Ru}(\text{bpy})_3]^{0/1-}$ (III)	-2135	-2095	-2180	-2115

for $[\text{R}_4\text{N}]_4[(\alpha\text{- or } \beta\text{-})\text{Mo}_{18}\text{O}_{54}(\text{SO}_3)_2]$ under the same conditions (Table 7). Again a series of poorly defined molybdenum redox processes was observed at more negative potentials. The potentials for molybdenum processes in $[\text{BMIM}][\text{PF}_6]$ follow the same order as in DMF (0.1 M Bu_4NPF_6) but occurred at significantly more positive potentials (by about 300–500 mV vs. Fc^+/Fc). At the very negative region of potential, the three reasonably well defined reduction processes (labelled as I, II and III in Fig. 10) represent the ligand based reductions of the $[\text{Ru}(\text{bpy})_3]^{2+}$ cation (Table 7).

Studies of the photo-electrochemical properties of the $[\text{Ru}(\text{bpy})_3][\text{Mo}_{18}\text{O}_{54}(\text{SO}_3)_2]^{4-}$ complex upon irradiation with white light in DMF, in the presence of 10% benzyl alcohol were conducted. However unlike the case with the W analogue, no stable $[\text{Mo}_{18}\text{O}_{54}(\text{SO}_3)_2]^{5-}$ or more reduced species was found, again illustrating the high level of reactivity of the reduced Mo system.

4. Conclusions

Voltammetric properties of the Dawson type sulfite polyoxometalate anions $[\text{M}_{18}\text{O}_{54}(\text{SO}_3)_2]^{4-}$ ($\text{M} = \text{Mo}, \text{W}$) containing R_4N or $[\text{Ru}(\text{bpy})_3]^{2+}$ cations have been surveyed in two organic solvents (DMF and CH_3CN) and in two ionic liquid media ($[\text{BMIM}][\text{PF}_6]$ and $[\text{BMIM}][\text{BF}_4]$). For solution studies in DMF only two polyoxometalate reduction processes were simple one electron steps. When the solid salts were adhered to the surface of a glassy carbon electrode in contact with ionic liquids they exhibited a further five ($\text{M} = \text{W}$) and two ($\text{M} = \text{Mo}$) well-defined one electron redox processes. The potentials for the polyoxometalate based redox processes in ionic liquids exhibited the same trends as in the organic solvents but occurred at hundreds of mV more positive potentials. In contrast the potentials of the $\text{Ru}^{3+/2+}$ and three or more bipyridyl ligand based reduction processes in $[\text{Ru}(\text{bpy})_3]^{2+}$ are not strongly dependent on the medium, which allowed voltammetric characterisation of the $[\text{Ru}(\text{bpy})_3]_2[\text{M}_{18}\text{O}_{54}(\text{SO}_3)_2]$ complexes ($\text{M} = \text{Mo}, \text{W}$) to be undertaken in the ionic liquids with minimal overlap of the extensive series of polyoxometalate and $\text{Ru}(\text{bpy})_3^{2+}$ processes. Even though an improvement in the $[\text{Ru}(\text{bpy})_3]_2[\text{M}_{18}\text{O}_{54}(\text{SO}_3)_2]$ (α and β isomer) electrochemistry in ionic liquid is also observed with respect to a series of one electron reduction steps when comparing to the behaviour in DMF, the voltammetric behaviour is never as extensive or as well defined as for the W analogue.

References

- C. Baffert, J. F. Boas, A. M. Bond, P. Kogerler, D.-L. Long, J. R. Pilbrow and L. Cronin, *Chem.–Eur. J.*, 2006, **12**, 8472–8483.
- D.-L. Long, P. Kogerler and L. Cronin, *Angew. Chem., Int. Ed.*, 2004, **43**, 1817–1820.
- N. Fay, A. M. Bond, C. Baffert, J. F. Boas, J. R. Pilbrow, D.-L. Long and L. Cronin, *Inorg. Chem.*, 2007, **46**, 3502–3510.
- C. Baffert, S. W. Feldberg, A. M. Bond, D.-L. Long and L. Cronin, *Dalton Trans.*, 2007, 599–4607.
- V. M. Hultgren, A. M. Bond and A. G. Wedd, *J. Chem. Soc., Dalton Trans.*, 2001, 1076–1082.
- N. Fay, V. M. Hultgren, A. G. Wedd, T. E. Keyes, R. J. Forster, D. Leane and A. M. Bond, *Dalton Trans.*, 2006, 4218–4227.
- N. Fay, E. Dempsey, A. Kennedy and T. McCormac, *J. Electroanal. Chem.*, 2003, **556**, 63–74.
- D.-L. Long, H. Abbas, P. Kögerler and L. Cronin, *Angew. Chem., Int. Ed.*, 2005, **44**, 3415–3419.
- P. Pearson, A. M. Bond, G. B. Deacon, C. Forsyth and L. Spiccia, *Inorg. Chim. Acta*, 2008, **361**, 601–612.
- J. Zhang, A. M. Bond, D. MacFarlane, S. A. Forsyth, J. M. Pringle, A. W. A. Mariotti, A. F. Glowinski and A. G. Wedd, *Inorg. Chem.*, 2005, **44**, 5123–2132 and references cited therein.
- S. K. Sukardi, J. Zhang, I. Burgar, M. D. Horne, A. F. Hollenkamp, D. R. MacFarlane and A. M. Bond, *Electrochem. Commun.*, 2008, **10**, 250–254.
- M. Takamoto, T. Ueda and S. Himeno, *J. Electroanal. Chem.*, 2002, **521**, 132–136.
- A. M. Bond, T. Vu and A. G. Wedd, *J. Electroanal. Chem.*, 2000, **494**, 96–104.
- S. Himeno and M. Takamoto, *J. Electroanal. Chem.*, 2000, **492**, 63–69.
- K. K. Kasem, *Electrochim. Acta*, 1996, **41**, 205–211.
- E. Itabashi, *Bull. Chem. Soc. Jpn.*, 1987, **60**, 1333–1336.
- B. Keita, D. Bouaziz and L. Nadjo, *J. Electrochem. Soc.*, 1988, **135**, 87.
- B. Keita and L. Nadjo, *J. Electroanal. Chem.*, 1987, **230**, 267.
- B. Keita and L. Nadjo, *J. Electroanal. Chem.*, 1987, **227**, 77.
- B. Keita and L. Nadjo, *J. Electroanal. Chem.*, 1987, **219**, 355.
- B. Keita and L. Nadjo, *J. Electroanal. Chem.*, 1987, **217**, 287.
- J. Zhang, A. M. Bond, P. J. S. Richardt, and A. G. Wedd, *Inorg. Chem.*, 2004, **43**, 8263–8271.
- Y. Ohsawa, K. W. Hanck and M. K. DeArmond, *J. Electroanal. Chem.*, 1984, **175**, 229–240.
- J. Zhang and A. M. Bond, *Anal. Chem.*, 2003, **75**, 6938–6948.
- T. Ruether, V. M. Hultgren, B. P. Timko, A. M. Bond, W. R. Jackson and A. G. Wedd, *J. Am. Chem. Soc.*, 2003, **125**, 10133–10143.
- A. M. Bond, D. M. Way, A. G. Wedd, R. G. Compton, J. Booth and J. C. Eklund, *Inorg. Chem.*, 1995, **34**, 3378–3384.
- A. M. Bond, J. C. Eklund, V. Tedesco, T. Vu and A. G. Wedd, *Inorg. Chem.*, 1998, **37**, 2366–2372.
- J. C. Eklund, A. M. Bond, D. G. Humphrey, G. Lazarev, T. Vu, A. G. Wedd and G. Wolfbauer, *J. Chem. Soc., Dalton Trans.*, 1999, 4373–4378.